



# Translational control of gene expression noise and its relationship to ageing in yeast

Tailise Carolina de Souza-Guerreiro, Xiang Meng, Estelle Dacheux , Helena Firczuk and John McCarthy 

Warwick Integrative Synthetic Biology Centre (WISB) and School of Life Sciences, University of Warwick, Coventry, UK

## Keywords

cell-to-cell heterogeneity; mRNA translation; replicative ageing; tracking senescing cells; yeast

## Correspondence

J. E. G. McCarthy, School of Life Sciences, University of Warwick, Gibbet Hill Campus, Coventry CV4 7AL, UK.  
Tel: +(0044) 2476528380  
Email: john.mccarthy@warwick.ac.uk

(Received 5 April 2020, revised 30 September 2020, accepted 7 October 2020)

doi:10.1111/febs.15594

Gene expression noise influences organism evolution and fitness but is poorly understood. There is increasing evidence that the functional roles of components of the translation machinery influence noise intensity. In addition, modulation of the activities of at least some of these same components affects the replicative lifespan of a broad spectrum of organisms. In a novel comparative approach, we modulate the activities of the translation initiation factors eIFG1 and eIF4G2, both of which are involved in the process of recruiting ribosomal 43S preinitiation complexes to the 5' end of eukaryotic mRNAs. We show that tagging of the cell wall using a fluorescent dye allows us to follow gene expression noise as different yeast strains progress through successive cycles of replicative ageing. This procedure reveals a relationship between global protein synthesis rate and gene expression noise (cell-to-cell heterogeneity), which is accompanied by a parallel correlation between gene expression noise and the replicative age of mother cells. An alternative approach, based on microfluidics, confirms the interdependence between protein synthesis rate, gene expression noise and ageing. We additionally show that it is important to characterize the influence of the design of the microfluidic device on the nutritional state of the cells during such experiments. Analysis of the noise data derived from flow cytometry and fluorescence microscopy measurements indicates that both the intrinsic and the extrinsic noise components increase as a function of ageing.

## Introduction

Ageing reflects the operation of mechanisms that have evolved to enable dividing cells to prevent the transfer of accumulated forms of damage to offspring [1–4]. Ageing in an asymmetrically dividing organism such as *Saccharomyces cerevisiae* therefore allows cell division to generate one rejuvenated cell (bud) whose lifespan is reset to its start point, plus one (mother) cell that retains damaged and functionally compromised molecular components that drive that cell towards senescence. *S.cerevisiae* is a valuable ageing model because many of the features of ageing observed in this organism are conserved in invertebrate species, rodents and

even man [4]. Of the factors that have been implicated in influencing longevity in yeast, a number are shared by higher organisms; these include dietary restriction [5], sirtuins [6], defective mitochondria [7], protein aggregates [8], oxidatively damaged (carbonylated) proteins [9] and extrachromosomal ribosomal DNA circles (ERCs) [10].

Moreover, in recent years evidence has been accumulating that cellular components influencing the translation of mRNA, such as the target of rapamycin (TOR; [11,12]) and the 60S subunit of the ribosome [13], can play a key role in determining organism

## Abbreviations

eIF, eukaryotic translation initiation factor; P-bodies, processing bodies.

longevity. Indeed, it is thought that, in yeast, the extension of longevity caused by dietary restriction is mediated via TOR signalling, which in turn suppresses ribosome protein production [4]. ERC formation may also be dependent on TOR activity [14]. Smith and colleagues [15] identified 25 homologue genes that affect lifespan in both *C. elegans* and *S. cerevisiae* – these included genes encoding ribosome proteins and translation initiation factors (eIFs), as well as TOR kinase (*TOR1*; *LET-363* in *C. elegans*) and ribosomal S6 kinase (*SCH9*; *RSKS-1* in *C. elegans*). Rapamycin, an inhibitor of the TOR kinase, extends lifespan in mice [16] and in *Schizosaccharomyces pombe* [12].

A striking aspect of the relationship reported between ribosome function and longevity is that mutations affecting 60S ribosomal subunits, but not mutations affecting 40S subunits, increase lifespan [13]. Moreover, the effect of 60S depletion on yeast longevity was reported to be largely dependent upon activation of *GCN4*, a gene whose encoded mRNA contains four upstream open reading frames (uORFs) that are involved in Gcn2-mediated translational up-regulation [13]. Yet, in other reported work, it was concluded that the lifespan of *C. elegans* is extended in response to inhibition of several translation initiation factors, including eIF4A, eIF4E, eIF4G, eIF5A and subunits of eIF2 and eIF3, (see above, as well as refs [15,17–20]). This is unexpected given that mutations in 40S subunits, which are involved in AUG scanning, were not observed to affect longevity [15], and that the inhibition of most eIFs is not known to cause depletion of 60S ribosomal subunits.

The fact that ageing is accompanied by different forms of molecular damage provides one potential reason why changes in gene expression stochasticity might occur during the course of an organism's lifespan [21]. There is little published work, and thus very limited knowledge, in this area. One report revealed a correlation between variance in the total expression per worm of a heat-shock *hfp-16.2::GFP* gene fusion and the longevity of *C. elegans* [22]. In another study, PCR amplification was used to detect increases in cell-to-cell variation in cardiomyocyte transcript abundance for a selection of genes as these cells age [23]. This latter study also found that oxidative damage increased gene expression variability. Other work based on RNA-sequencing indicated that ageing increases expression heterogeneity resulting from immunological activation of mouse cells [24]. Further studies have reported that haploid yeast cells expressing the yellow fluorescent protein (YFP) gene from the inducible  $P_{GALI}$  promoter manifested time-dependent ('intracellular') noise that decreased with age [25], whereas cell-to-cell

heterogeneity in expression of the green fluorescent protein (GFP) gene from the constitutive  $P_{TEFI}$  promoter in diploid cells was found to increase with age [26].

Recent research has examined the relationship between protein synthesis activity and the nongenetic cell-to-cell variation associated with gene expression noise [27,28]. Modulation of the activity of the highly conserved translation initiation factor eIF4G1 was found both to suppress global translation and to increase the expression noise for the eIF4G-encoding gene in yeast [27]. In other words, cell-to-cell variation in the cellular content of this factor is highly sensitive to the rate at which it is synthesized. This is relevant to observations that eIF4G activity influences replicative lifespan in worms [29,30] and yeast [15]. Moreover, gene expression noise was also found to increase upon insertion of inhibitory secondary structures into the 5'-untranslated regions of mRNAs in yeast [28]. Here, we have extended these observations by, first, exploring the relationship between ageing and gene expression noise (manifested as cell-to-cell heterogeneity) in yeast and, second, by determining the influence of restricting translation on noise in ageing cells. The results provide evidence of an interdependence between global translation, gene expression noise and ageing.

## Results

### Imaging fluorescence-tagged mother cells over multiple generations

Our objective was to characterize the progression of gene expression noise generation (in a timescale that is detectable as the cell-to-cell heterogeneity of production of a reporter protein) as a function of the replicative age status of *Saccharomyces cerevisiae*. This required that we track ageing mother cells over multiple generations as they generate a series of daughter cells over time. We performed a one-off labelling of a number of exponentially growing yeast strains (carrying a genomic yEGFP reporter gene expression construct; see next section) using the fluorescent dye Alexa 555. After washing, the labelled mother cells retained the fluorescent dye while they continued to divide, generating daughter cells bearing newly synthesized, and thus unlabeled, cell walls (Figs. 1 and 2A–F). This meant that we could use flow cytometry to analyse differentially the cell-to-cell heterogeneity in the expression of yEGFP in the originally labelled mother cells as these aged over time. In order to seek unequivocal evidence that the Alexa 555-labelled cells were a

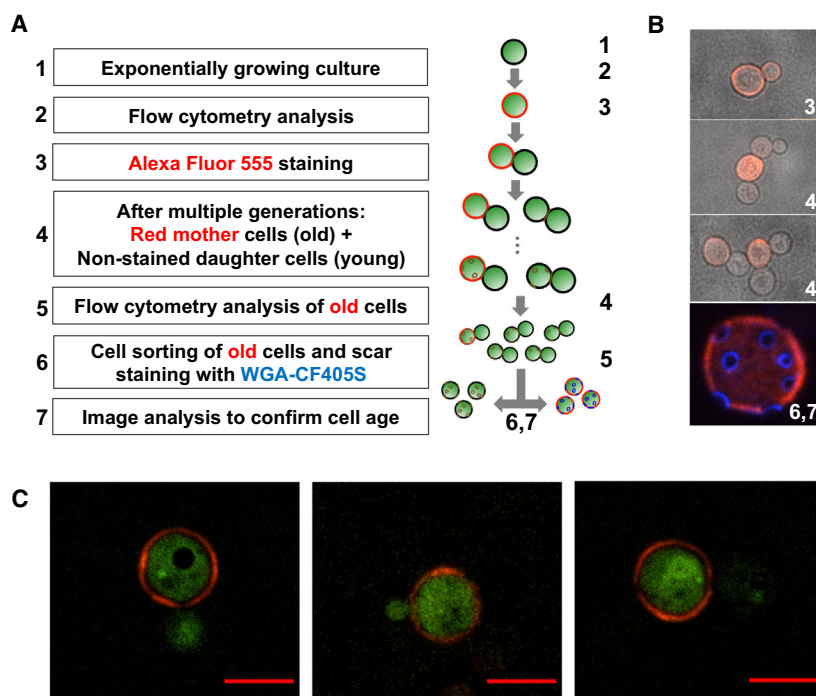


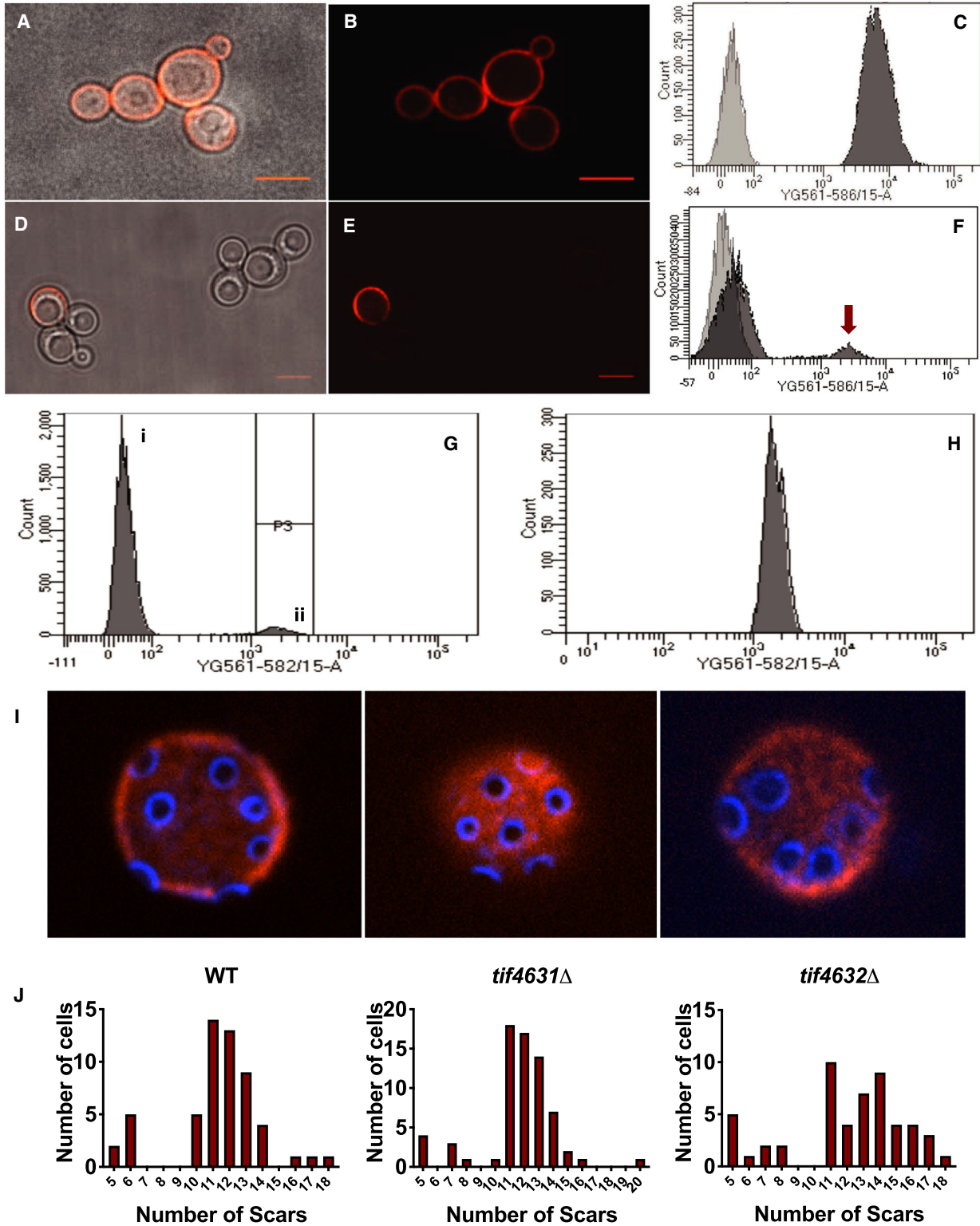
**Fig. 1.** Monitoring of ageing mother cells in exponentially growing yeast cells. The scheme shows the workflow for cell-wall tagging and analysis (A), accompanied by representative images of cell staining corresponding to the respective stages in the workflow (B). In the example shown here, a culture of strain PTC41 was allowed to reach exponential growth (stage 1) and the cells were monitored using fluorescence microscopy and flow cytometry (stage 2) before and after cell-wall staining was performed using Alexa 555 (stage 3). The *tif4631Δ* strain (PTC444) grew more slowly (see Fig. S2), and therefore, longer growth periods were required to enable it to reach the same cell density as the wild-type reference strain PTC41. After further growth (stage 4), culture samples were again monitored using flow cytometry (stage 5) and, at the chosen growth stage, the population was subjected to cell sorting (stage 6). The aged mother cells selected in this way were stained with WGA-CF405S, and the bud scar counts were determined using fluorescence confocal microscopy (stage 7). Further images of typical single cells at generation 11 (C) illustrate simultaneous detection of yEGFP expression and Alexa 555 staining. Background fluorescence was subtracted using a rolling ball radius of 120 pixels. The scale bar represents 5  $\mu\text{m}$ .

defined and stable population undergoing normal replicative ageing, we analysed the cells using flow cytometry and isolated the red-fluorescing cells using a cell sorter (Fig. 2G,H). Staining of the cells isolated in this way using Wheat Germ Agglutinin (WGA) CF-405S conjugate allowed us to quantitate the number of scars in the cell wall, thus revealing the number of buds generated by each cell during its lifetime (Fig. 2I). The scar counts were subjected to statistical analysis (Fig. 2J), thus providing accurate information on the average age of the cells under study. Individual cell cycle times vary considerably (as also observed previously by others [31]), and consequently, we observed a broad distribution of cell ages in these experiments. Alternative cell-wall dyes (e.g. Alexa 700, also employed in this study; see Supporting information section) can be used in this procedure, thus allowing the application of this strategy in combination with a range of different cytoplasmic reporters. This means

that a number of combinations of alternative reporter proteins and cell-wall-labelling dyes can be utilized in this approach.

### The relationship between replicative ageing and gene expression noise

Each of the strains studied in this work contained a genomic yEGFP expression construct (Fig. 3A; Figure S1) that included a constitutive promoter ( $P_{TEF1}$ ), thus allowing us to assess how ageing affects gene expression noise under a range of conditions. The  $P_{TEF1}$  promoter was chosen because it lacks a TATA box, an element that has been shown to contribute to increased noise levels by influencing transcriptional burst size [32,33]. yEGFP expression was studied in cells labelled using Alexa 555 according to the protocol described above (Fig. 1C). The expression constructs used in this work are listed in Table S1.



We performed flow cytometry on three different yeast strains: a reference ('wild-type') strain (PTC41) with no mutation in either of the eIF4G-encoding genes; a PTC41-derivative strain with a deletion of the gene encoding eIF4G1 (*tif4631Δ*; PTC444); and a PTC41-derivative strain with a deletion of the gene encoding eIF4G2 (*tif4632Δ*; PTC507). eIF4G1 was chosen because this is a high-flux-control factor that plays a major role in translation initiation, while eIF4G2 serves as a useful low-flux-control comparator [34]. As expected, deletion of eIF4G1 (*tif4631Δ*) was found to result in a reduced growth rate (compare ref [34] and see Fig. S2). The flow cytometry data generated in the experiments that we describe below were subjected to a previously published type of analysis [35] that assesses how the noise varies as a function of the gating radius centred at the point of highest cell density (see examples of the resulting plots in Fig. 3B, C).

The type of analysis used here provides an overview of the heterogeneity of gene expression and of cell size and composition in each cell population. Plotting forward scattering vs side scattering data (Fig. 3B,C) reflects cell size and composition heterogeneity, including the inevitable detection of both single cells and 'doublets' (caused by pairs of normally single cells, or any aggregated cells remaining after sonication, passing through the cytometer detection system; see Fig. 3 G,H for a more detailed analysis of how we are able to exclude the influence of cell doublets). Gene expression stochasticity is generally regarded as comprising

two components: intrinsic noise that is attributed to inherent stochasticity of expression from a specified gene system, and extrinsic noise that results from fluctuations in the intracellular environment, for example linked to the cell cycle and/or changes in the capacity of the expression machinery. The total noise squared ( $\eta_{\text{tot}}^2$ ) is thought to equate to the sum of the squared values of the intrinsic and extrinsic noise components  $\eta_{\text{int}}^2 + \eta_{\text{ext}}^2$  [38]. The gating analysis procedure enabled us to identify the trend in noise as a function of decreasing overall cell-to-cell heterogeneity (see, e.g., Fig. 3B,C). This facilitated the process of determining CV% values that had reduced contributions from extrinsic noise factors (see the vertical dotted lines in the plot in Fig. 3B,C).

To begin with, we measured yEGFP fluorescence in exponentially growing cells of the 'wild-type' strain bearing no translation factor mutations. It is estimated that approximately 80% of cells in a log-phase culture are newborn and 12% have budded just once [36,37], so the vast majority (~92%) of the cells studied in this way were at generation 1 or 2. After the cell-wall staining protocol, cells were allowed to continue growth up to a mean age of 11 generations. Flow cytometric analysis was then used to extract the yEGFP data generated by the older subset of cells on the basis of their Alexa 555 fluorescence which, at this stage, comprised a greatly reduced proportion of the total population (Fig. 2H). This enabled us to identify an increase in the gene expression noise in wild-type cells as the stained cells progressed through the ageing

**Fig. 2.** Cell-wall staining. These images illustrate how cell-wall staining remains associated with the initially stained (mother) cells through multiple divisions. Immediately after staining using Alexa 555, fluorescence microscopy reveals that all cells are stained (the example here shows PTC41 cells observed with and without bright field; A,B). Flow cytometry confirms complete labelling; the dark grey peak corresponds to cells manifesting high-intensity red fluorescence (C; typical microscopy images are shown), as observed in stages 2 and 3 in the scheme shown in Fig. 1. Continued growth yields a population in which the majority of cells are not labelled and a minority still manifest intense red fluorescence from their cell walls. This is illustrated here using cells that have progressed through a further 5 divisions, by which time the stained mother cells already represent a small percentage of the total cell population (D,E; hundreds of images of stained cells were collected, of which illustrative examples are presented in panels A, B, D and E). The small subpopulation of strongly fluorescing aged mother cells is also evident in the flow cytometry analysis (small dark grey peak on the right in panel F; indicated by the arrow; see also panels G and H below). A substantial number of the younger cells have retained a small amount of staining (dark grey peak on the left in panel F), but remain readily distinguishable from the fully stained mother cells. The light grey peaks in panels C and F represent low-intensity yeast cell autofluorescence. Panels G and H illustrate the selection of aged mother cells via cell sorting. A culture of cells was subjected to fluorescence-activated cell sorting (FACS) after the equivalent of 5 average doubling times (G). Sorting was triggered in response to Alexa 555 signal intensity. The cell sorter readily distinguishes between those cells manifesting high-intensity fluorescence (ii) and younger cells that have only low levels of fluorescent dye (i). After FACS, the sorted cells (ii) were reanalysed via flow cytometry to verify correct and complete sorting of aged mother cells (H). Note the different scales on the respective y-axes. We confirmed cell ages by staining bud scars (I). Here, we show images of individual yeast cells from an Alexa 555-stained subpopulation (average age of 11 generations). Samples of the sorted cells were treated with Wheat Germ Agglutinin (WGA) CF-405S conjugate, and observed under a confocal microscope (excitation 405nm, detection using a 447/60 filter). Analysis of multiple cells (J) revealed bud scar counts as follows: WT:  $n = 55$ , average = 11.4; *tif4631Δ*:  $n = 69$ , average = 11.7; *tif4632Δ*:  $n = 52$ , average = 12.1.

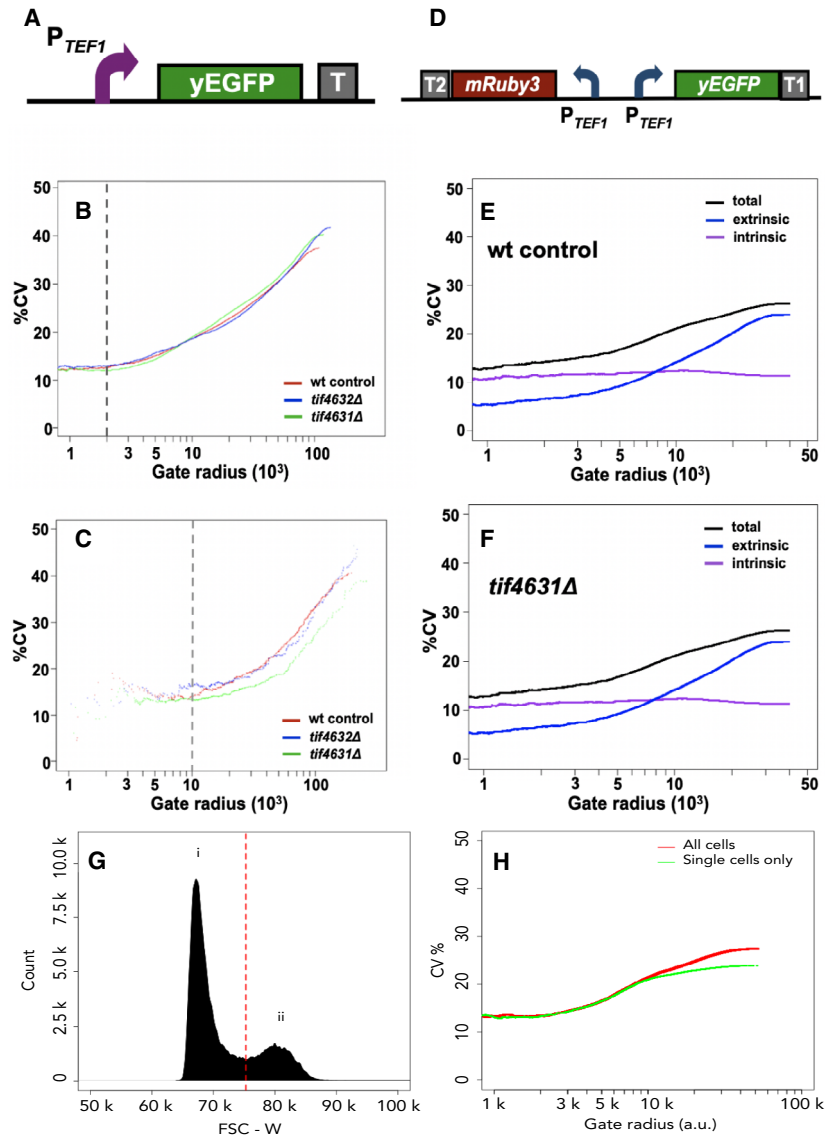


**Fig. 3.** Flow cytometry analysis of genomic reporter gene expression. (A) Gene expression noise was determined using a genomically integrated yEGFP reporter construct. This construct was transcribed from the  $P_{TEF1}$  promoter, and transcription was terminated at a downstream  $PGK1$  terminator (T). (B) Typical gate radius vs CV% plot for cell populations of mean age 1 of the three strains indicated in the panel. As described previously (35), progressively constraining the heterogeneity of the cells (reducing the gate radius) included in the reporter fluorescence intensity analysis (i.e. moving right to left along the gate radius axis) progressively reduces the contribution of extrinsic noise factors and reduces the overall CV% value (it also largely excludes doublets; see panels G,H). In each case, the point at which the CV% value had reached a minimum is indicated by a vertical broken line, and this value was taken as the gated noise estimate for that particular experiment (and included in the data summarized in Figure 4). (C) Typical gate radius vs CV% plot for cell populations of mean age 11 of the three strains indicated in the panel. The individual plots for the aged cells were considerably noisier than for complete populations of exponentially growing cells because of the greatly reduced proportion of cells in the aged subpopulations (see Fig. 2F). Reliable mean CV values were obtained by analysing the results of multiple experiments (see Supporting Information section). The intrinsic and extrinsic noise components could be more precisely distinguished using a genomically integrated dual-reporter construct (D), which allows direct comparison of expression of the two reporter proteins in each cell. This approach was successfully applied to populations of exponentially growing (average generation 1) cells of the wild-type (E) and *tif4631Δ* (F) strains; for these cells, a gate radius of 2k was used as the reference point for determining the estimates for intrinsic, extrinsic and total noise, respectively.

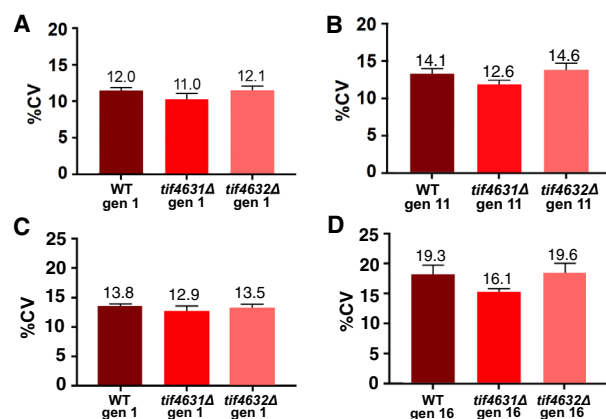


**Fig. 4.** Gene expression noise as a function of replicative age, estimated on the basis of gate-radius-dependent analysis of flow cytometry data. The CV% bar graphs show average values of the respective sets of biological repeats and are arranged in two pairs: values for cell populations at mean generation 1 (A) and then for the same populations at mean generation 11 (B); values for cell populations at mean generation 1 (C) and then for the same populations at mean generation 16 (D). The relevant statistical values for these graphs are presented in the text. *t*-Test analysis was performed for each strain to investigate the significance of the increase in noise level over the ageing process. One-way ANOVA was performed to analyse the significance of the difference observed between young populations of the three strains analysed, as well as the significance of the difference observed between old populations of the three strains analysed. Whiskers indicate the standard deviation values. The data shown in panels A and B were derived from three biological repeats, while the data shown in panels C and D were derived from four biological repeats.

process (compare Fig. 3B,C, Fig. 4A,B, also Tables S2 and S3).

Accordingly, the CV% values summarized in Fig. 4 correspond to the points at which the CV% vs gate radius plots (see, e.g., Fig. 3B,C) had decreased to a plateau – that is at which a minimum point of heterogeneity had been reached. There is an increase in the estimated intrinsic gene expression noise in the cells of all strains analysed as they age, and a *t*-test analysis shows that for the wild-type and *tif4632Δ* strains, this age-dependent increase is statistically significant (WT  $P = 0.013$ ; *tif4632Δ*  $P = 0.017$ ). For the *tif4631Δ* strain, which has the smallest increase in the estimated level of noise during the ageing process, the age-dependent increase is not statistically significant ( $P = 0.053$ ). Indeed, the *tif4631Δ* strain at the 11<sup>th</sup>-generation stage (Fig. 4B) manifests the lowest CV% value compared with 11th-generation WT and *tif4632Δ* strains. At this age, one-way ANOVA reveals a statistically significant difference between the CV% values for the respective strains ( $P = 0.039$ ).

We also analysed cells that had grown to a mean age of 16 generations (Fig. 4C,D). At this point, the proportion of cells in the overall population that were in the selected age range was so small that we were approaching the feasible limit of analysis. We observed a continuing trend of increasing noise with age, whereby a *t*-test analysis shows that for each strain the increase in the noise level over the ageing process is statistically significant (WT  $P = 0.0005$ ; *tif4631Δ*  $P = 0.0008$ ; *tif4632Δ*  $P = 0.0004$ ). For the 16th-generation analysis, populations showed a significant statistical difference in the value of CV% ( $P = 0.009$ ). The post hoc Tukey's analysis test showed that the *tif4631Δ* strain differs significantly from both wild-type and *tif4632Δ* strains ( $P < 0.05$ ); the wild-type and *tif4632Δ* strains, on the other hand, do not differ significantly from each other. The experimental data are tabulated in full in the Supporting Information section.

At the same time, we observed that more variations in features including cell size and heterogeneity in structural composition became evident within the greatly reduced population sizes for aged cells (see, e.g., the right-hand side of the plots in Fig. 3C). Therefore, in the light of these results, we sought to add more precision to the distinction between intrinsic and extrinsic components of gene expression noise by using the previously described dual-reporter strategy ([38]; and compare our application of this procedure to yeast in [28]), which relies on measurement of the ratio between two reporter constructs (Fig. 3D). The dual-reporter construct used for this work (pJM1233; Fig. S3) included bacteriophage MS2 coat protein binding sites in the 3'UTR downstream of the yEGFP reporter gene. At least under certain experimental conditions (e.g. mRNAs overproduced from plasmids, coexpression of the bacteriophage MS2 coat protein and glucose starvation), the introduction of MS2 binding sites has previously been found to affect mRNA stability, and we have provided a more detailed consideration of these potential effects in the Supporting Information section. However, we note that our dual-reporter mRNAs were expressed from a single-copy genomic integration construct in a strain that was neither coproducing the MS2 coat protein nor subject to glucose starvation. In addition, any modulation of the stability of the yEGFP mRNA caused by the presence of the MS2 binding elements would be expected to result in a constant ratio of steady-state reporter expression under any given set of growth conditions, and thus not to affect the analysis of noise carried out here.

For this part of the work, cell-wall staining was performed using Alexa 700 since this does not overlap significantly with the excitation/emission spectra of

mRuby3. We found that this procedure provided a clearer picture of the respective noise components, at least for the overall population of exponentially growing cells (Fig. 3E). The results allowed us to estimate the intrinsic and extrinsic noise values for 1<sup>st</sup>-generation cells of the wild-type strain (mean intrinsic =  $9.6\% \pm 1.0\%$ ; mean extrinsic =  $6.4\% \pm 1.4\%$ ). These data confirm that the dual-reporter method separates the intrinsic and extrinsic noise components more effectively than the gating radius cell selection technique. However, we were unable to obtain reproducible estimates of the intrinsic and extrinsic noise components by applying the dual-reporter approach to the subpopulations of average age 11th and 16th generations, primarily because of the very small numbers of cells. This prompted us to turn to the use of a microfluidics technique to provide further information about the properties of older cells (see later section).

### Translation rate is a modulating influence on age-dependent gene expression noise

As considered above, we have found that the cell-wall-staining method allows us to monitor cell-to-cell heterogeneity as a function of replicative age. Considering further the influence of changes in the activity of the two isomers of the eukaryotic initiation factor 4G (eIF4G1 and 2), we can see that the gate radius method (as illustrated in Fig. 3F) indicates that *tif4631Δ* cells of average age generation 1 manifest a slightly reduced gated noise level relative to cells whose translation rate is not restricted by reduced eIF4G activity (Fig. 4A,C). In contrast, the *tif4632Δ* strain manifests no such effect. The latter result constitutes a valuable control, since it has been shown previously that removal of eIF4G2 alone has at most a minor effect on translation rate and thus on growth rate ([34] and Fig. S1).

It is evident that the *tif4631Δ* mutation markedly limits the impact of ageing on gene expression noise. Remarkably, the loss of eIF4G1 activity has only a minimal effect on intrinsic and extrinsic noise components in 'young' cells (Fig. 3E,F) but does suppress noise in cell subpopulations averaging 11 generations in age (Fig. 4B), and this becomes even more marked in cells that have an average age of 16 generations (Fig. 4D). The lack of impact of the deletion of *tif4632* is maintained throughout. Moreover, the dual-reporter strategy revealed that the *tif4631Δ* strain (Fig. 3F) shows a very similar split between intrinsic and extrinsic noise (mean intrinsic =  $9.4\% \pm 0.6\%$ ; mean extrinsic =  $6.5\% \pm 0.6\%$ ) to that seen in the wild-type strain (Fig. 3E). We therefore conclude that

the inhibition of translation caused by deletion of eIF4G1 counteracts the progressive increase in noise that is otherwise observed as cells progress towards a higher replicative age.

### Monitoring ageing and gene expression noise in a microfluidic cell

It is evident from the above experimental work that selecting cells analysed by flow cytometry according to gate radius allows us to reduce the complexity of the cell populations under study, largely by excluding doublets and limiting variations in cell volume and cellular structural features that affect light scattering. This approach generates highly reproducible expression noise estimates from which much of the extrinsic noise has been removed. In addition, utilizing the dual-reporter technique, we have been able to determine, on a cell-by-cell basis, the relationship between intrinsic and extrinsic noise components, albeit only for younger cells.

While recognizing the above as an informative platform for assessing the relationships between ageing, gene expression noise and translation activity, we wanted to investigate an alternative (and complementary) experimental strategy in order to assess whether this might contribute to a more holistic understanding of the contributions of extrinsic and intrinsic noise components. Microfluidic devices have recently been introduced as a platform for studying (single) cells whose growth can be supported by the constant exchange of growth medium, and we wanted to compare the suitability of this approach with the cell-staining strategy described above. We chose to use a previously described design for a microfluidic device [39] (Fig. 5A) that features finger-shaped traps that facilitate the tracking of individual cells as the population expands as the result of budding (Fig. 5B–E). Utilizing this alternative method, we obtained results that were consistent with the data generated using the cell-labelling procedure. However, we noted that the difference in estimated noise levels determined for the wild-type and *tif4631Δ* strains, respectively, was greater when studying cells in the microfluidic system (Fig. 6). This was at least partly due to the fact that the noise estimates obtained in this way reflected both the intrinsic and extrinsic components of cell-to-cell heterogeneity in the studied strains. At the same time, we were also aware of the possibility that the microfluidic device environment might itself influence the outcomes of our measurements. We therefore investigated the role played by the microfluidic device in more detail.



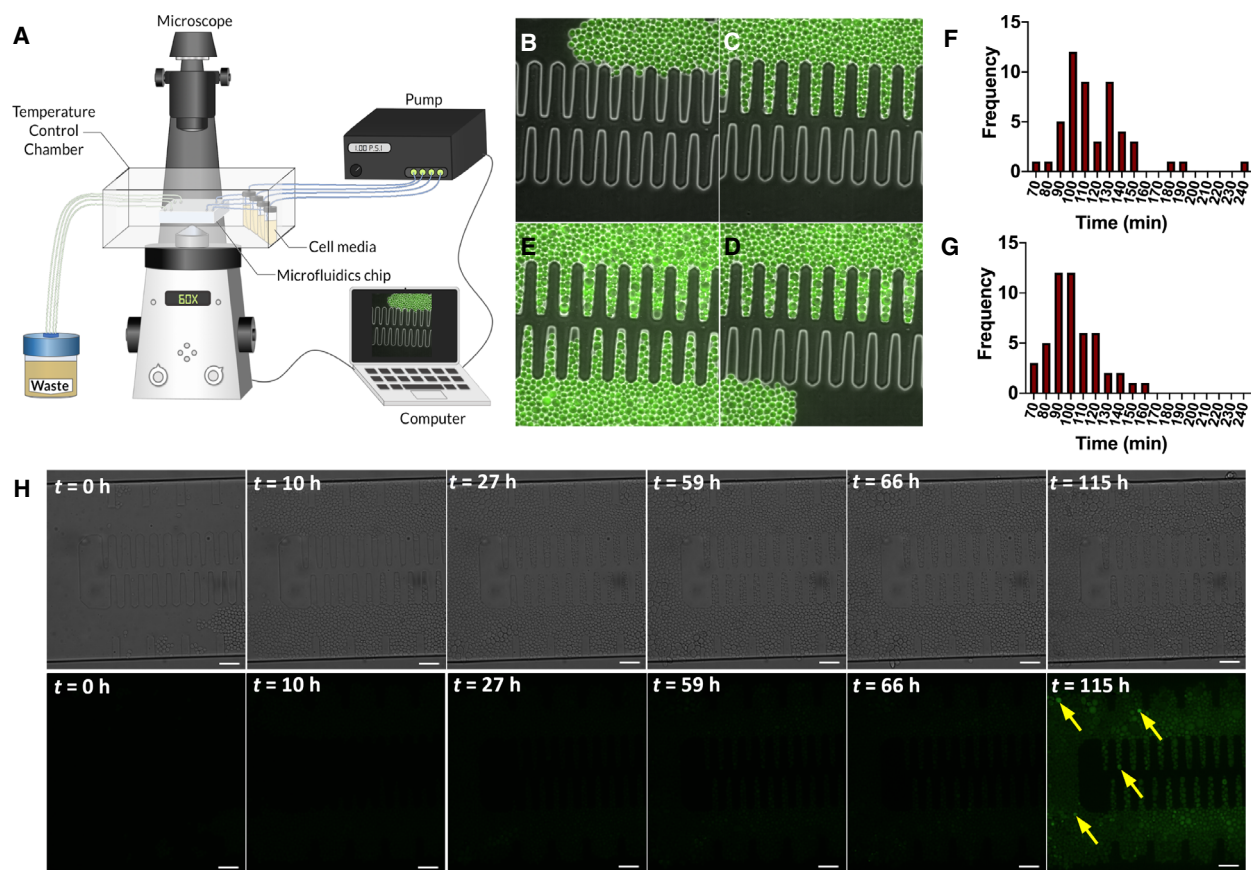


**Fig. 5.** Studying yeast cells in the microfluidic finger trap device. (A) Scheme showing the arrangement of the microfluidic system components. (B–E) Ingress of exponentially growing cells into the microfluidic device, each panel showing different time points of observation of the same device. As the cell numbers increase through budding, the cells move progressively deeper into the respective finger-shaped channels. Cell cycle duration (doubling) times for individual cells were determined for cells within (F) and outside (G) the finger traps. The resulting histograms show that for cells within the finger traps (F): mean = 117 min; median = 110 min;  $n = 50$ ; for cells outside the finger traps (G): mean = 100 min; median = 98 min;  $n = 50$ . We also show fluorescence microscopy images taken of one batch of yeast cells in the finger trap microfluidics cell at different time points (H). Here, we used a derivative of PTC 41 containing a genomic integration encoding an Edc3::ymNeonGreen protein fusion, that acts as a marker for P-bodies. No P-bodies were detectable under the conditions of the stochasticity experiments described in this study, which were completed within 90 h of initiating the time-lapse. Where time-lapse imaging was allowed to continue significantly beyond this period (up to 115 h), a small number of P-bodies became evident in some cells (see arrows in  $t = 115$ h frame).

Since the tracked cells moved progressively deeper into the finger-shaped traps, we performed control experiments in order to determine whether the rate of movement of growth medium through the microfluidic device was sufficient to sustain a consistent rate of exponential reproduction and whether the cells were subject to nutritional stress. In our view, this supplementary assessment is essential to enable a reliable interpretation of the data obtained using such a device. First, we measured the average cell-cycle time (i.e. time from one budding event to the next) before and after they entered the finger-shaped traps. We found that the average cell-cycle duration was 17% longer for

cells within the finger traps than for cells outside of the traps (Fig. 5F,G) if growth medium was pumped through the device at the maximum pressure of 0.9psi. Second, we checked whether the cells in the finger-shaped traps manifested stress-induced P-bodies, since these are known to be generated in response to glucose starvation [40]. We observed no formation of P-bodies within cells in the microfluidic device during the period of the noise vs ageing experiments, even in those located deep within the finger-shaped traps (Fig. 5H). Overall, these experiments revealed that yeast cells are subjected to a mild degree of nutritional limitation within the traps, but no evidence of nutritional stress

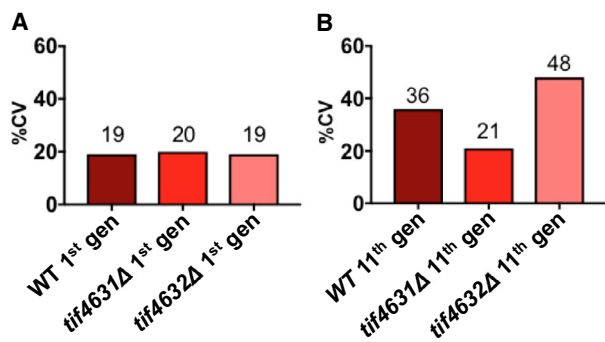


**Fig. 6.** Gene expression noise values for cells studied in the microfluidic system. The plots compare the CV% values of cell populations at mean generation points 1 (A) and 11 (B) for the wild-type, *tif4631Δ* and *tif4632Δ* strains, respectively. The data presented here are based on measurements performed on 100 cells of each strain.

(although P-bodies did begin to form after longer periods of incubation in the microfluidics cell; see  $t = 115h$  panel in Fig. 5H).

Having characterized the impact on the growth and nutritional growth response of yeast cells when they enter the finger-like traps of the microfluidic device, we proceeded to study the fluorescence intensity generated by the expression of the respective genomic GFP reporter strains over the time-course of replicative ageing. Significant differences in cell-to-cell heterogeneity became apparent over the course of eleven generations (Fig. 6), confirming the two general trends identified using the flow cytometry measurements described above. First, gene expression noise increased with replicative age. Second, the deletion of eIF4G1 at least partially suppressed this age-dependent increase in gene expression noise. At the same time, we note that the changes observed using the microfluidics-based measurements were quantitatively more marked than those observed in the flow cytometry experiments. Our additional investigations suggest that these quantitative differences are likely to be at least partially attributable to a combination of two things: (i) the fact that the CV values determined using the microfluidic device are the sum of intrinsic and extrinsic noise components; (ii) the condition of nutritional limitation that applies when the cells are cultured in the microfluidic environment.

## Discussion

In this study, we have used two parallel experimental strategies to explore the three-component relationship

between global translation rate, replicative lifespan and gene expression noise in *Saccharomyces cerevisiae*. Reporter gene transcription has been driven by a constitutive promoter in cells performing multiple cell cycles within a narrowly defined phase of exponential growth. We have used a comparative approach of benchmarking the age-related noise characteristics of a strain lacking the eIF4G1 isomer with those of a wild-type strain and of a strain that has a *tif4632Δ* deletion. This provides unequivocal evidence of a relationship between global translation rate and gene expression noise. The cell-wall-staining approach we have described is found to be an effective and relatively efficient strategy for performing age-related gene expression studies, obviating the need to perform the labour- and time-intensive manual separation of mother and daughter cells using a micromanipulator. For comparative purposes, we also explored the same relationship within the environment of a microfluidic device. This was of particular interest because of the growing number of studies that have used microfluidic systems for the study of microbial populations.

By looking for signs of nutritional limitation and determining the rate of progression of individual cells through the cell cycle, we have been able to conclude that the cells within the microfluidic system we have used are subject to some degree of limitation of access to glucose. This limitation reduces the growth of cells but does not elicit a starvation response. Under these conditions, we have observed that the influence of ageing on gene expression noise follows the same trend as we have identified when studying cell populations using flow cytometry, whereby the quantitative impact measured in the microfluidic system is greater. This accentuated sensitivity to ageing is consistent with a previously reported observation that gene expression noise increases in nutrient-deficient cells [41], although we do not know whether the effect we see in this study is fully equivalent to that described previously. However, at the same time, it is important to note that the procedure used to measure cell-to-cell heterogeneity in the microfluidic system generates CV values that include intrinsic and extrinsic noise values.

In summary, we conclude that the study of cells within this microfluidic system provides confirmation of the general positive relationship between age and gene expression noise, but our investigations also indicate that it would be wise, for the sake of transparency, for users of microfluidic devices to characterize the influence of this type of environment on the nutritional state of the cells. Overall, the factors discussed above can explain a large part of the observed difference in magnitude of the impact of the

*tif4631Δ* deletion between the two experimental methods. At the same time, it is important to emphasize that the microfluidics experiments were exploratory in the sense that, at this stage, no attempt was made to perform a statistically underpinned quantitative analysis of gene expression noise with this system. This was because, while the microfluidic data revealed a consistent overall trend in gene expression noise as a function of age, the results also indicated that more time and effort will need to be invested in identifying optimal, fully defined, experimental conditions for such systems.

The observation that age-dependent gene expression noise is reduced in a strain whose translation machinery activity is constrained by deletion of the *TIF4631* gene (encoding eIF4G1) raises the question as to the mechanistic basis of the apparent relationship between protein synthesis and stochasticity. One potentially relevant effect of attenuated translation activity is that this may reduce the rate of production of misfolded proteins which, in turn, can be expected to partially suppress the accumulation of intracellular damage, especially in the form of oxidatively damaged proteins (23). Moreover, the limitation of translation might also result in additional energy resources being made available for cellular maintenance and repair processes. This possibility has been considered previously in relation to data indicating that model organisms with reduced protein synthesis had increased stress resistance and longer lifespan [42,43]. It is possible that cells with enhanced energy resources available for cell maintenance might better control the gene expression process, which could in principle result in reduced noise, but further studies will be required to test this hypothesis.

On the other hand, one previous report concluded [25] that gene expression noise decreases during the ageing process. It is important to note that this earlier study used microfluidics to study heterogeneity in yeast cells expressing YFP controlled by the regulatable  $P_{GAL}$  promoter. Remarkably, the same group reported an age-dependent increase in gene expression noise for a constitutively expressed construct ( $P_{TEFI}$ -ssGFP; a GFP isoform with a shorter half-life) in diploid cells [26]. The most likely explanation of the markedly different results obtained with the respective promoters is that a distinct mechanism (or a distinct balance of mechanisms) of noise generation is associated with the regulatable  $P_{GAL}$  promoter and the specific growth conditions under which it can be used. This might be linked to regulation-dependent variations in alternative nucleosome configurations associated with this

promoter [44], whereby these variations could undergo modulation or suppression as a function of age.

Comparison with the effects of changes imposed on signalling pathways that impact upon protein synthesis is informative. For example, it has been found that inhibition of the target of rapamycin (TOR) pathway [45,46] results in extended lifespan. Rapamycin is thought to induce modulation of the phosphorylation state of several different factors that influence translation initiation and may also influence elongation via an analogous mechanism [47], whereby it has been argued that inhibition of elongation increases translational accuracy [48]. Other work has shown that ageing can be affected by increased translational inaccuracy because this interferes with protein folding [49]. However, inhibition of TOR by rapamycin, such as caloric restriction, also induces autophagy, and it has been proposed that enhanced autophagy plays a role in extending longevity [50]. One way in which autophagy could prolong lifespan is by virtue of the fact that it helps clear aggregates containing damaged proteins (which have the potential to adversely affect gene expression machinery functionality, and thus noise). In this context, it is valuable to note that elevation of ubiquitin/proteasome system (UPS) activity in yeast by increasing the abundance of the UPS-related transcription factor Rpn4 results in extended lifespan [51]. This is consistent with the earlier observed correlation between oxidative damage and gene expression noise in cardiomyocytes [23].

In this work, we have inhibited protein synthesis directly by limiting the availability of one of the

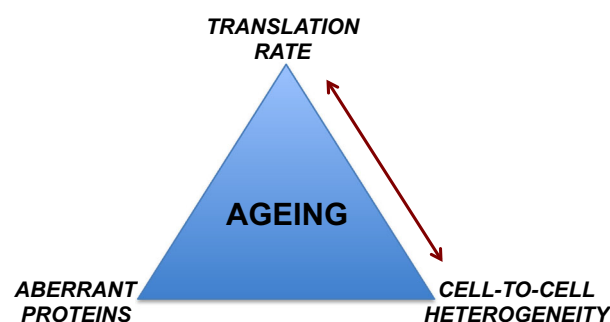


**Fig. 7.** Ageing is modulated by interrelationships between multiple processes. Taking together, the results from this and other studies suggest a scheme of relationships involving gene expression stochasticity (cell-to-cell heterogeneity), protein synthesis rate and aberrant proteins (erroneous in terms of structure, modifications, folding and/or abundance). The current study characterizes, in *S. cerevisiae*, the relationship along the axis: translation rate–replicative ageing–cell-to-cell heterogeneity.

components of the translation machinery. It seems to us that the results presented here, together with previously published work (e.g. [23,49–53]), suggest an interpretation in terms of a set of relationships (Fig. 7) between gene expression stochasticity (cell-to-cell heterogeneity), aberrant proteins (erroneous in terms of structure, modifications, folding and/or abundance) and translation, whereby the present study has focused on the axis: translation rate – replicative ageing – cell-to-cell heterogeneity. It is noteworthy that attenuation of multiple translation initiation factors extends the lifespan of *C.elegans* [15,17–20]. Moreover, experimentally imposed suppression of the abundance of the equivalent set of factors in *S.cerevisiae* has been demonstrated to markedly inhibit global protein synthesis [34]. Collectively, these observations support the argument that the global protein synthesis rate is a major determinant of ageing rate in multiple organisms.

Also of relevance to our study is that a previous characterization of the wider transcriptome and proteome in yeast as a function of ageing led to the conclusion that the latter becomes progressively decoupled from the former [52], in the sense that encoded proteins become increasingly overrepresented relative to their corresponding mRNAs in the cell. This again suggests how translation might contribute to the accumulation of damaged proteins over time, and thus to the intensification of noise generation. It naturally follows from this line of reasoning that the inhibition of protein synthesis (e.g. by limiting eIF4G activity) could be expected to both suppress noise generation and extend lifespan. In general terms, proteostasis is thought to be maintained by a fine balance between protein synthesis, chaperone-mediated protein folding, autophagy and proteasomal degradation, and any distortion of the relationship between these processes can potentially affect ageing [53].

Finally, a number of recent studies have highlighted how the relationship between translational control and gene expression noise has wider significance in terms of human health. A striking feature of these studies has been the accumulating evidence that aberrant intracellular levels of translation factors correlate with cell transformation and tumour development [54]. eIF4G1, for example, is overproduced in nasopharyngeal carcinoma, squamous cell lung carcinoma and breast cancer, and an abnormal abundance of this factor is regarded as a predictor of inflammatory breast cancer [55]. Moreover, excess synthesis of eIF4G1 has been reported to induce tumour transformation in mouse fibroblasts [46]. Other research has pointed to a correlation between cancer and gene expression noise.

Analysis of transcriptomic data from cancers in human liver, colon, lung and breast tissues revealed that gene expression noise for many genes was increased when compared to normal tissues [56]. In addition, more than 53% of genes in that study were found to display increased stochasticity in patients with late stage, as opposed to early-stage cancer, suggesting that accuracy in gene expression may influence the cancer outcome. Overall, these and other results are consistent with the existence of a chain of intercausality between aberrant translation factor abundance, anomalous gene expression noise, cellular ageing and cancer. Moreover, it is also noteworthy that gene expression stochasticity within the multinucleated syncytium of the mouse myofibre is also impacted by the maturation process, thus linking gene expression noise to development [60]. This wider perspective emphasizes the importance of pursuing further research on the molecular basis of the relationships between translational control, ageing and noise using a range of exemplar organisms.

## Materials and Methods

### Strain construction

The haploid strains used in this study were developed in the *S. cerevisiae* W303 background (MAT $\alpha$  *ade2-1 ura3-1 leu2-3,112 his3-11,15 can1-100*; referred to here as PTC 41). Each of the eIF4G-isomer-encoding genes was previously knocked out in this strain to produce the derivative strains *tif4631 $\Delta$  (PTC 444) and *tif4632 $\Delta$  (PTC 507) [27,34]. A genomic yEGFP expression construct was integrated into all three of these strains at the *HIS3* locus, using a plasmid (pNM1-*HIS*; Fig. S2) containing the *HIS3* gene (allowing auxotrophic selection) or the *KanMX* gene (encoding resistance to G418) and the fluorescent reporter flanked by regions homologous to the 5' and 3' regions of the yeast *HIS3* open reading frame. A different plasmid (pJM1233; Fig. S3) was used for the dual-reporter experiments. The plasmids, which also included bacteriophage MS2 coat protein stem-loop structures (see Supporting Information), were digested using ApaI or BglI restriction enzymes (depending on the reporter), cutting outside of the inserted sequence. The linearized plasmids were used for yeast transformation (integration by homologous recombination) following an adapted version of a previously published protocol [57].**

### Microfluidics

The microfluidic chip master was made using standard soft lithography techniques (with the support of M. Polin, University of Warwick Physics Department). Polydimethylsiloxane (PDMS) (Sylgard 184) was poured over the master

and cured to produce the microchannels. The PDMS piece was then covalently bound to a coverslip using a plasma cleaner (Harrick Plasma). Since this equipment uses low pressure to generate plasma, a RC.8D vacuum pump (D.V.P. vacuum technology) was used for 1–3 min to evacuate the air inside the chamber and the resulting partial vacuum was maintained until the end of procedure. Oxygen was used as the processing gas. High radio frequency (RF) irradiation was used for 1–2 min to create radicals on both the PDMS chip and glass coverslip surfaces. The PDMS chip was placed on top of a glass coverslip, and the assembled microfluidic device was placed on a heating block (60 °C–80 °C) for at least one hour. Construction of the microfluidic cell followed a previous design [39].

### Time-lapse image acquisition

High-resolution time-lapse microscopy of yeast cells growing in constantly flowing medium (0.9–1.0 psi) in the microfluidics chip installed inside a cage incubator (Okolab) at 30 °C was performed using a Nikon TI-E Eclipse motorized wide-field epifluorescence microscope equipped with an EMCCD or sCMOS camera (Andor) and a 60x oil immersion objective. Yeast was grown in yeast nitrogen base synthetic medium (YNB), either lacking histidine (single fluorescent reporter experiments) or complete (dual-reporter experiments). Bright field or phase-contrast images were acquired at intervals between 10 to 12 min, with GFP excitation ( $\lambda_{\text{ex}} = 488 \text{ nm}$ ) being induced at regular intervals set at between 12 and 60 min. Total time-lapse duration varied between 90 and 115 h. A CellASIC® ONIX Microfluidic Platform was used to regulate and maintain the medium flow pressure.

### Image analysis

Microscopy images of the microfluidic device were analysed using the ImageJ (v2.0 National Institutes of Health) software package to count the number of daughter cells produced by a single mother cell and to measure fluorescence intensity. Each newborn cell was identified, and an outline was drawn around the cell as a measure to enable us to capture its fluorescence intensity. Manual tracking of this cell was then performed until the 10th bud (11th generation) was produced, and an outline was again drawn around the aged cell. This process was repeated for at least 100 cells of each strain analysed. Integrated density, mean fluorescence, plus the minor and major ellipsoidal axes, and background readings were determined.

### Cell-wall labelling, flow cytometry analysis and cell sorting

We performed cell-wall staining using a modified version of a previously described protocol [58]. Yeast cells were

cultured at 30 °C overnight and were then diluted in the morning to  $\text{OD}_{600} = 0.01\text{--}0.02$  and incubated for 8–10 h, until  $\text{OD}_{600} = 0.4\text{--}0.7$  was attained. The cells were diluted once more in fresh medium to  $\text{OD}_{600} = 0.0001\text{--}0.0002$  and cultivated overnight, thus maintaining the cells in exponential growth. The following day, cells were diluted to  $\text{OD}_{600} = 0.1\text{--}0.2$  and incubated for 3–5 h to reach  $\text{OD}_{600} = 0.4\text{--}0.6$ . About 1 mL of cells was harvested by centrifugation and washed with PBS, and the cell walls were stained for 10 min at 30 °C by adding 250  $\mu\text{L}$  of 26.7 mM Alexa 555-NHS ester/PBS solution (or an alternative dye solution). After staining, cells were washed twice with PBS, resuspended in culture media, diluted to a predicted density equivalent to  $\text{OD}_{600} = 0.0001\text{--}0.0002$  and incubated at 30 °C for 16–19 h to allow the cells to replicate for an average of 10 times. For the analysis of bud scars, a sample was collected and subjected to fluorescence-activated cell sorting (FACS) to separate old mother cells. In order to study mother cells that had completed an average of 15 budding events, cell suspensions were serially diluted to a predicted density equivalent to  $\text{OD}_{600} = 0.0001\text{--}0.0002$  with the objective of ensuring that the cultures remained in exponential phase throughout all stages of preparation for the experiments. A BD Biosciences Fortessa flow cytometer was used to measure GFP (B488-530/30-A) and Alexa 555 (YG561-586/15-A) signals and a BD Biosciences FACSaria Fusion was used to measure the same signals and to sort cells according to their Alexa 555 fluorescence level. In most cases, short bursts of sonication of cell samples (for a total period of up to one minute) were applied prior to flow cytometry in order to disperse aggregates. If larger sample volumes (containing more cells) were used, the sonication time was extended as required, and the exclusion threshold for yEGFP fluorescence values was adjusted if necessary. Flow cytometry of dual-reporter strains and the analysis of the data generated from them were performed as described previously [28]. The cell walls of dual-reporter strains were stained using Alexa 700 to avoid overlap of the cell-wall stain fluorescence spectrum with the mRuby3 fluorescence spectrum. Cells manifesting an intensity value  $\geq 10^3$  for Alexa 555 or Alexa 700 were included in the data analysis.

### WGA-conjugate scar staining and microscopy

Following a protocol based on a previously described method [59], cells selected by the cell sorter were subjected to scar staining using Wheat Germ Agglutinin (WGA) CF-405S conjugate. The cells were collected by centrifugation, washed twice with PBS and stained in 250  $\mu\text{L}$  of 100  $\mu\text{g}/\text{mL}$  WGA CF-405S – PBS solution (incubation tube covered with foil and rocked gently at 30 °C for 30 min). The stained cells were then washed twice with PBS and studied by fluorescence microscopy. Slides were prepared for microscopy analysis using anti-fade mounting medium, following

the manufacturer's protocol (Vectashield HardSet, Vector Labs). Images were acquired using a Nikon TI-E Eclipse motorized spinning disc confocal microscope equipped with an EMCCD camera (Andor) and a 100× oil immersion objective. For each cell, multiple images were taken at different focal distances to build a composite image that would allow counting of bud scars.

## Acknowledgements

We thank Marco Polin (Physics Dept, University of Warwick) and Ollver Sinfield (Life Sciences Dept, University of Warwick) for advice on the preparation of microfluidic devices; Oliver Sinfield also kindly provided the EDC3::ymNG fusion construct. We are also grateful to the Research Technology Facility (managed by Sarah Bennett) of the Warwick Integrative Synthetic Biology centre (WISB), and the University of Warwick Life Sciences support (including media production) technical staff. This work was supported, at different stages of its development, by the Biotechnology & Biological Sciences Research Council through a Fellowship grant (BB/E024181/1) and two project grants (BB/1020535/1 and BB/1008349/1). It also benefited from access to the Research Technology Facility of the Warwick Integrative Synthetic Biology centre (WISB), which received funding from EPSRC and BBSRC (BB/M017982/1). TCdS was the beneficiary of a PhD scholarship from CAPES (Coordenação de Aperfeiçoamento de Pessoal de Nível Superior – Brazil).

## Conflicts of interest

The authors declare no conflict of interest.

## Author contributions

JEGM designed the study. TCSG with the support of XM, ED and HF performed experiments. JEGM wrote the manuscript.

## References

- Steinkraus KA, Kaeberlein M & Kennedy BK (2008) Replication aging in yeast: the means to the end. *Annu Rev Cell Dev Biol* **24**, 29–54.
- Ackermann M, Chao L, Bergstrom CT & Doebeli M (2007) On the evolutionary origin of aging. *Aging Cell* **6**, 235–244.
- Erjavec N, Cvijovic M, Klipp E & Nyström T (2008) Selective benefits of damage partitioning in unicellular systems and its effects on aging. *Proc Natl Acad Sci USA* **105**, 18764–18769.
- Kaeberlein M (2010) Lessons on longevity from budding yeast. *Nature* **464**, 513–519.
- Kennedy BK, Steffen KK & Kaeberlein M (2007) Ruminations on dietary restriction and aging. *Cell Mol Life Sci* **64**, 1323–1328.
- Kaeberlein M, McVey M & Guarente L (1999) The SIR2/3/4 complex and SIR2 alone promote longevity in *Saccharomyces cerevisiae* by two different mechanisms. *Genes Dev* **13**, 2570–2580.
- Payne BAI & Chinnery PF (2015) Mitochondrial dysfunction in aging: much progress but many unresolved questions. *Biochim Biophys Acta* **1847**, 1347–1353.
- Saarikangas J & Barral Y (2015) Protein aggregates are associated with replicative aging without compromising protein quality control. *eLife* **4**, e06197.
- Pérez VI, Buffenstein R, Masamsetti V, Leonard S, Salmon AB, Mele J, Andziak B, Yang T, Edrey Y, Friguet B *et al*, (2009) Protein stability and resistance to oxidative stress are determinants of longevity in the longest-living rodent, the naked mole-rat. *Proc Natl Acad Sci USA* **106**, 3059–3064.
- Ganley AR, Ide S, Saka K & Kobayashi T (2009) The effect of replication initiation on gene amplification in the rDNA and its relationship to aging. *Mol Cell* **35**, 683–693.
- Powers RW III, Kaeberlein M, Caldwell SD, Kennedy BK & Fields S (2006) Extension of chronological life span in yeast by decreased TOR pathway signalling. *Genes Dev* **20**, 174–184.
- Rallis C, Codlin S & Bähler J (2013) TORC1 signalling inhibition by rapamycin and caffeine affect lifespan, global gene expression, and cell proliferation of fission yeast. *Aging Cell* **12**, 563–573.
- Steffen KK, MacKay VL, Kerr EO, Tsuchiya M, Hu D, Fox LA, Dang N, Johnston ED, Oakes JA, Tchao BN *et al*, (2008) Yeast life span extension by depletion of 60S ribosomal subunits is mediated by Gcn4. *Cell* **133**, 292–302.
- Riesen M & Morgan A (2009) Calorie restriction reduces rDNA recombination independently of rDNA silencing. *Aging Cell* **8**, 624–632.
- Smith ED, Tsuchiya M, Fox LA, Dang N, Di Hu, Kerr EO, Johnston ED, Tchao BN, Pak DN, Welton KL *et al*, (2008) Quantitative evidence for conserved longevity pathways between divergent eukaryotic species. *Genome Res* **18**, 564–570.
- Harrison DE, Strong R, Sharp ZD, Nelson JF & Miller RA (2009) Rapamycin fed late in life extends lifespan in genetically heterogeneous mice. *Nature* **460**, 392–395.
- Syntichaki P, Troulinaki K & Tavernarakis N (2007) eIF4E function in somatic cells modulates ageing in *Caenorhabditis elegans*. *Nature* **445**, 922–926.
- Pan KZ, Palter JE, Rogers AN, Olsen A, Chen D, Lithgow GJ & Kapahi P (2007) Inhibition of mRNA

- translation extends lifespan in *Caenorhabditis elegans*. *Aging Cell* **6**, 111–119.
- 19 Hansen M, Taubert S, Crawford D, Libina N, Lee SJ & Kenyon C (2007) Lifespan extension by conditions that inhibit translation in *Caenorhabditis elegans*. *Aging Cell* **6**, 95–110.
  - 20 Chen D, Pan KZ, Palter JE & Kapahi P (2007) Longevity determined by developmental arrest genes in *Caenorhabditis elegans*. *Aging Cell* **6**, 525–533.
  - 21 Raj A & Oudenaarden A (2008) Nature, nurture, or chance: stochastic gene expression and its consequences. *Cell* **135**, 216–226.
  - 22 Rea SL, Wu D, Cypser JR, Vaupel JW & Johnson TE (2005) A stress-sensitive reporter predicts longevity in isogenic populations of *Caenorhabditis elegans*. *Nat Genet* **37**, 894–898.
  - 23 Bahar R, Hartmann CH, Rodriguez KA, Denny AD, Busuttill RA, Dollé ME, Calder RB, Chisholm GB, Pollock BH, Klein CA & *et al*, (2006) Increased cell-to-cell variation in gene expression in ageing mouse heart. *Nature* **441**, 1011–1014.
  - 24 Martinez-Jimenez CP, Eling N, Chen H-C, Vallejos CA, Kolodziejczyk AA, Connor F, Stojic L, Rayner TF, Stubbington MJT, Teichmann SA *et al*, (2017) Aging increases cell-to-cell transcriptional variability upon immune stimulation. *Science* **355**, 1433–1436.
  - 25 Liu P, Song R, Elison GL, Peng W & Acar M (2017) Noise reduction as an emergent property of single-cell aging. *Nat Commun* **8**, 680.
  - 26 Sarnoski EA, Song R, Ertekin E, Koonce N & Acer M (2018) Fundamental characteristics of single-cell aging in diploid yeast. *iScience* **7**, 96–109.
  - 27 Meng X, Firczuk H, Pietroni P, Westbrook R & McCarthy JEG (2016) Minimum-noise production of translation factor eIF4G maps to a mechanistically determined optimal rate control window for protein synthesis. *Nucleic Acids Res* **45**, 1015–1025.
  - 28 Dacheux E, Malys N, Meng X, Ramachandran V, Mendes P & McCarthy JEG (2017) Translation initiation events on structured eukaryotic mRNAs generate gene expression noise. *Nucleic Acids Res* **45**, 6981–6992.
  - 29 Curran SP & Ruvkun G (2007) Lifespan regulation by evolutionarily conserved genes essential for viability. *PLoS Genet* **3**, e56.
  - 30 Rogers AN, Chen D, McColl G, Czerwieńiec G, Felkey K, Gibson BW, Hubbard A, Melov S, Lithgow GJ & Kapahi P (2011) Life span extension via eIF4G inhibition is mediated by posttranscriptional remodeling of stress response gene expression in *C elegans*. *Cell Metab* **14**, 5–66.
  - 31 di Talia S, Skotheim JM, Bean JM, Siggia ED & Cross FR (2007) The effects of molecular noise and size control on variability in the budding yeast cell cycle. *Nature* **448**, 947–951.
  - 32 Murphy KF, Adams RM, Wang X, Balázs G & Collins JJ (2010) Tuning and controlling gene expression gene expression noise in synthetic gene networks. *Nucleic Acids Res* **38**, 2712–2726.
  - 33 Blake WJ, Balázs G, Kothanski MA, Isaacs FJ, Murphy KF, Kuang Y, Cantor CR, Walt DR & Collins JJ (2006) Phenotypic consequences of promoter-mediated transcriptional noise. *Mol Cell* **24**, 853–865.
  - 34 Firczuk H, Kannambath S, Pahle J, Claydon A, Beynon R, Duncan J, Westerhoff H, Mendes P & McCarthy JEG (2013) An *in vivo* control map for the eukaryotic mRNA translation machinery. *Mol Syst Biol* **9**, 1–13.
  - 35 Newman JR, Ghaemmaghami S, Ihmels J, Breslow DK, Noble M, DeRisi JL & Weissman JS (2006) Single-cell proteomic analysis of *S cerevisiae* reveals the architecture of biological noise. *Nature* **441**, 840–846.
  - 36 Jo MC, Liu W, Gu L, Dang W & Qin L (2015) High-throughput analysis of yeast replicative aging using a microfluidic system. *Proc Natl Acad Sci USA* **112**, 9364–9369.
  - 37 Lee SS, Vizcarra IA, Huberts DHEW, Lee LP & Heinemann M (2012) Whole lifespan microscopic observation of budding yeast aging through a microfluidic dissection platform. *Proc Natl Acad Sci USA* **109**, 4916–4920.
  - 38 Elowitz MB, Levine AJ, Siggia ED & Swain PS (2002) Stochastic gene expression in a single cell. *Science* **297**, 1183–1186.
  - 39 Fehrmann S, Paoletti C, Goulev Y, Ungureanu A, Aguilaniu H & Charvin G (2013) Aging yeast cells undergo a sharp entry into senescence unrelated to the loss of mitochondrial membrane potential. *Cell Rep* **5**, 1589–1599.
  - 40 Teixeira D, Sheth U, Valencia-Sanchez MA, Brengues M & Parker R (2005) Processing bodies require RNA for assembly and contain nontranslating mRNAs. *RNA* **11**, 371–382.
  - 41 Keren L, van Dijk D, Weingarten-Gabbay S, Davidi D, Jona G, Weinberger A, Milo R & Segal E (2015) Noise in gene expression is coupled to growth rate. *Genome Res* **25**, 1893–1902.
  - 42 Hipkiss AR (2007) On why decreasing protein synthesis can increase lifespan. *Mech Ageing Dev* **128**, 412–414.
  - 43 Tavernarakis N (2008) Ageing and the regulation of protein synthesis: A balancing act? *Trends in Cell Biol* **18**, 228–235.
  - 44 Brown CR & Boeger H (2014) Nucleosomal promoter variation generates gene expression noise. *Proc Natl Acad Sci USA* **111**, 17893–17898.
  - 45 Ramírez-Valle F, Braunstein S, Zavadil J, Formenti SC & Schneider RJ (2008) eIF4GI links nutrient sensing by mTOR to cell proliferation and inhibition of autophagy. *J Cell Biol* **181**, 293–307.

- 46 Howard A & Rogers AN (2014) Role of translation initiation factor 4G in lifespan regulation and age-related health. *Ageing Res Rev* **13**, 115–124.
- 47 Raught B, Gingras A-C & Sonenberg N (2001) The target of rapamycin (TOR) proteins. *Proc Natl Acad Sci USA* **98**, 7037–7044.
- 48 Conn CS & Qian S-B (2013) Nutrient signaling in protein homeostasis: an increase in quantity at the expense of quality. *Sci Signal* **6**, 1–9.
- 49 von der Haar T, Leadsham JE, Sauvadet A, Tarrant D, Adam IS, Saromi K, Laun P, Rinnerthaler M, Breitenbach-Koller H, Breitenbach M *et al.* (2017) The control of translational accuracy is a determinant of healthy ageing in yeast. *Open Biology* **7**, 160291.
- 50 Rubinsztein DC, Mariño G & Kroemer G (2011) Autophagy and aging. *Cell* **146**, 682–695.
- 51 Kruegel U, Robison B, Dange T, Kahlert G, Delaney JR, Kotireddy S, Tsuchiya M, Tsuchiyama S, Murakami CJ, Schleit J *et al.* (2011) Elevated proteasome capacity extends replicative lifespan in *Saccharomyces cerevisiae*. *PLoS Genet* **7**, e1002253.
- 52 Janssens GE, Meinema AC, González J, Wolters JC, Schmidt A, Guryev V, Bischoff R, Wit EC, Veenhoff LF & Heinemann M (2015) Protein biogenesis machinery is a driver of replicative aging in yeast. *eLife* **4**, 1–24.
- 53 Hipp MS, Kasturi P & Hartl FU (2019) The proteostasis network and its decline in ageing. *Nat Rev Mol Cell Biol* **20**, 421–435.
- 54 de la Parra C, Walters BA, Geter P & Schneider RJ (2018) Translation initiation factors and their relevance in cancer. *Curr Opin Genet Dev* **48**, 82–88.
- 55 Fukuchi-Shimogori T, Ishii I, Kashiwagi K, Mashiba H, Ekimoto H & Igarashi K (1997) Malignant transformation by overproduction of translation initiation factor eIF4G. *Cancer Res* **57**, 5041–5044.
- 56 Han R, Huang G, Wang Y, Xu Y, Hu Y, Jiang W, Wang T, Xiao T & Zheng D (2016) Increased gene expression noise in human cancers is correlated with low p53 and immune activities as well as late stage cancer. *Oncotarget* **7**, 72011–72020.
- 57 Güldener U, Heck S, Fiedler T, Beinhauer J & Hegemann JH (1996) A new efficient gene disruption cassette for repeated use in budding yeast. *Nucleic Acids Res* **24**, 2519–2524.
- 58 Yang J, McCormick MA, Zheng J, Xie Z, Tsuchiya M, Tsuchiyama S, El-Shahd H, Ouyang Q, Kaerberlein M, Kennedy BK & *et al.* (2015) Systematic analysis of asymmetric partitioning of yeast proteome between mother and daughter cells reveals “aging factors” and mechanism of lifespan asymmetry. *Proc Natl Acad Sci USA* **112**, 11977–11982.
- 59 Patterson MN & Maxwell PH (2014) Combining magnetic sorting of mother cells and fluctuation tests to analyze genome instability during mitotic cell aging in *Saccharomyces cerevisiae*. *J Visualized Exp* **16**, e51850.
- 60 Newlands S, Levitt LK, Robinson CS, Karpf AB, Hodgson VR, Wade RP & Hardeman EC (1998) Transcription occurs in pulses in muscle fibers. *Genes Dev* **12**, 2748–2758.

## Supporting information

Additional supporting information may be found online in the Supporting Information section at the end of the article.

**Fig. S1.** Plasmid map of pNM1-HIS.

**Fig. S2.** Growth rates of respective yeast strains.

**Fig. S3.** Plasmid map of pJM1233.

**Table. S1.** Expression constructs used in this work.

**Table. S2.** Summary of genomic yEGFP expression data comparing 1st generation and 11th generation cells (3 biological repeats).